Endoplasmic Reticulum

Mass Balance and Surface Proteins

SIAM Life Science – MS 8

Aug 6, 2018

Keith Promislow
Federica Brandizzi, Noa Kraitzman, Brian Wetton

Hydrophobic verses Amphiphilic Interactions

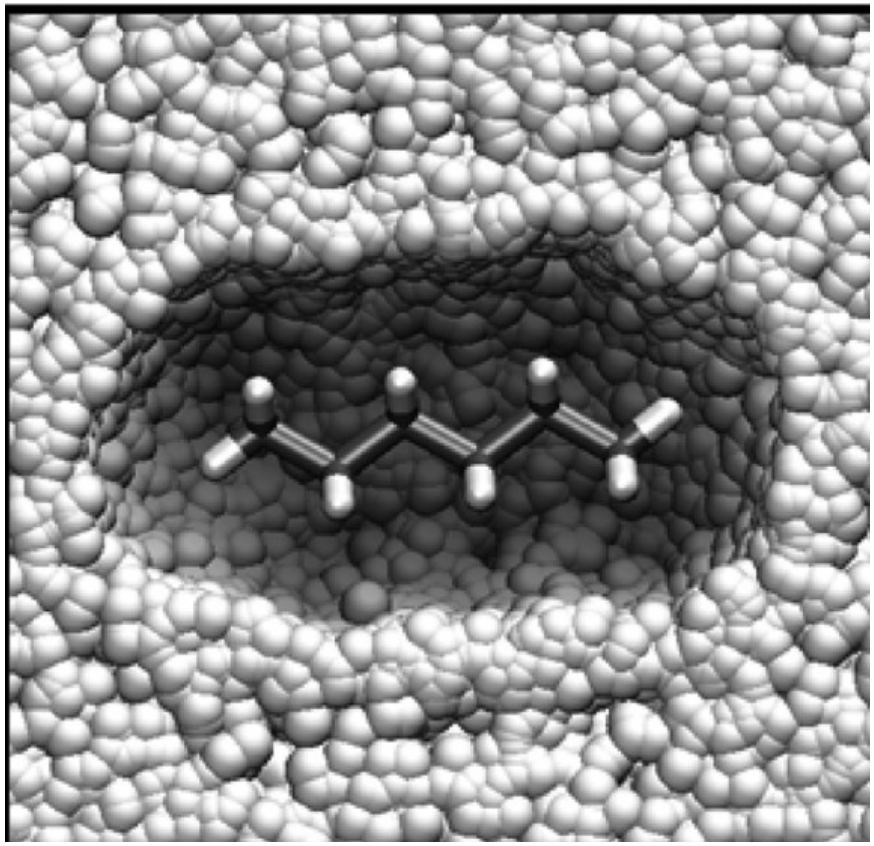

Codimension: 3 micelles, 2 filaments, 1 bilayer

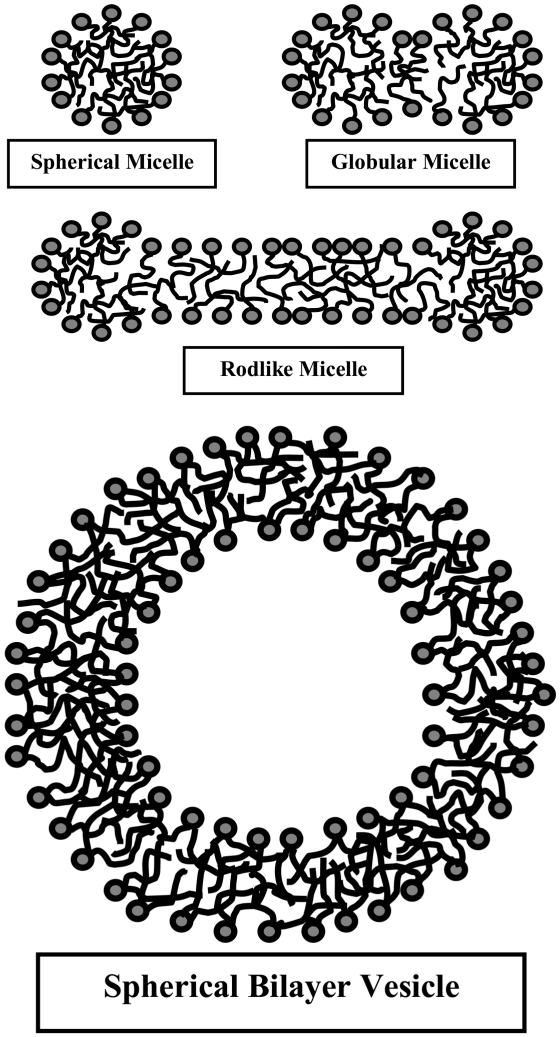

Hydrophobic interactions, oil in water produces an excluded region or vacuum with very high energy density. **Amphiphilic** materials pack a hydrophobic tail within a volume lined with hydrophilic head groups.

Amphiphilic Materials: Aspect Ratio, Packing, and Codimension

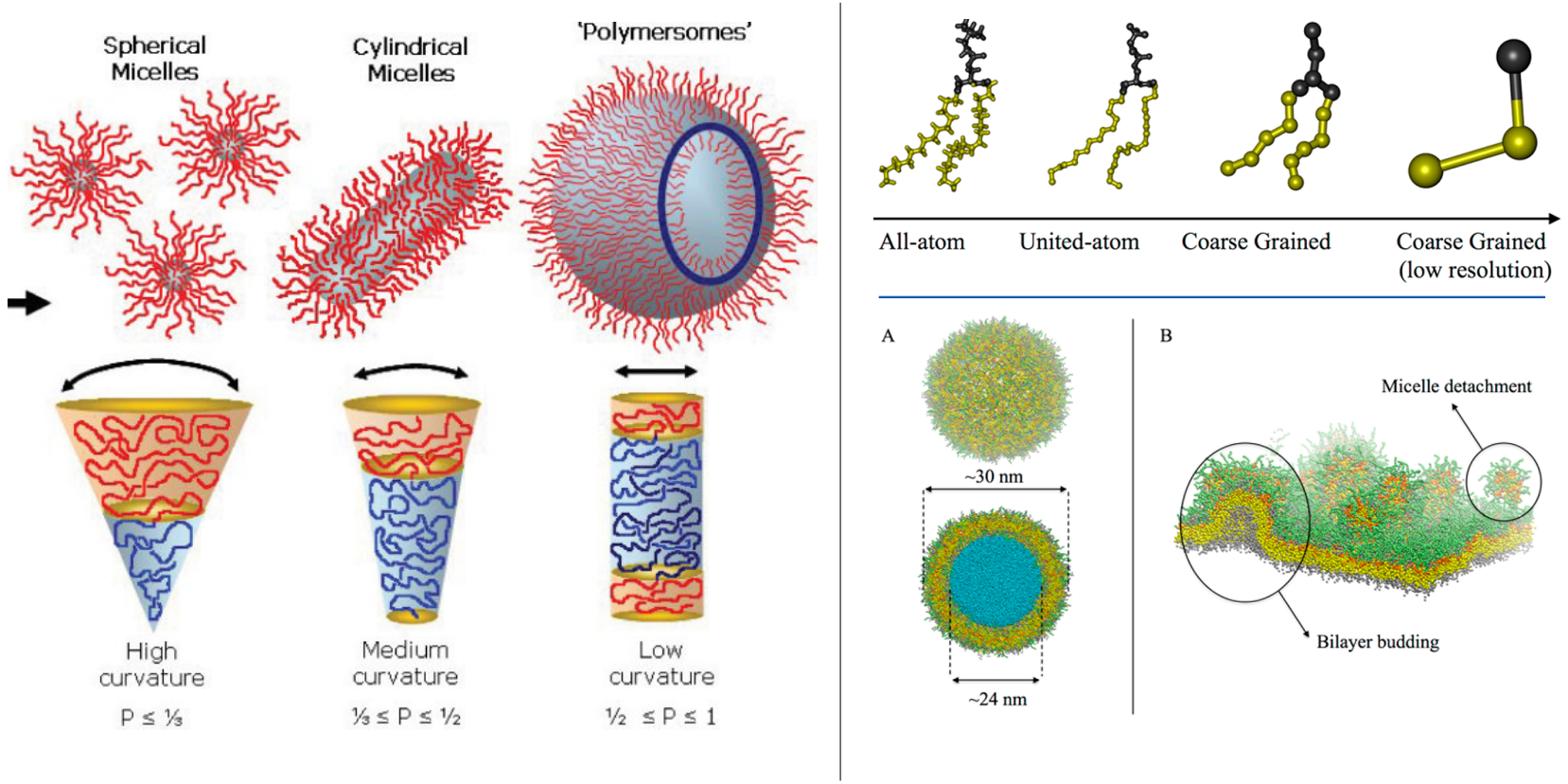

(left) Amphiphilic polymers: relation of aspect ratio to codimension in amphiphillic diblocks Blanazs (2009). (right) Course-graining of atomistic models of lipids, MD simulations of budding and micelle detachment using implicit solvent.

Endoplasmic Reticulum (ER): Cisternea and Tubules

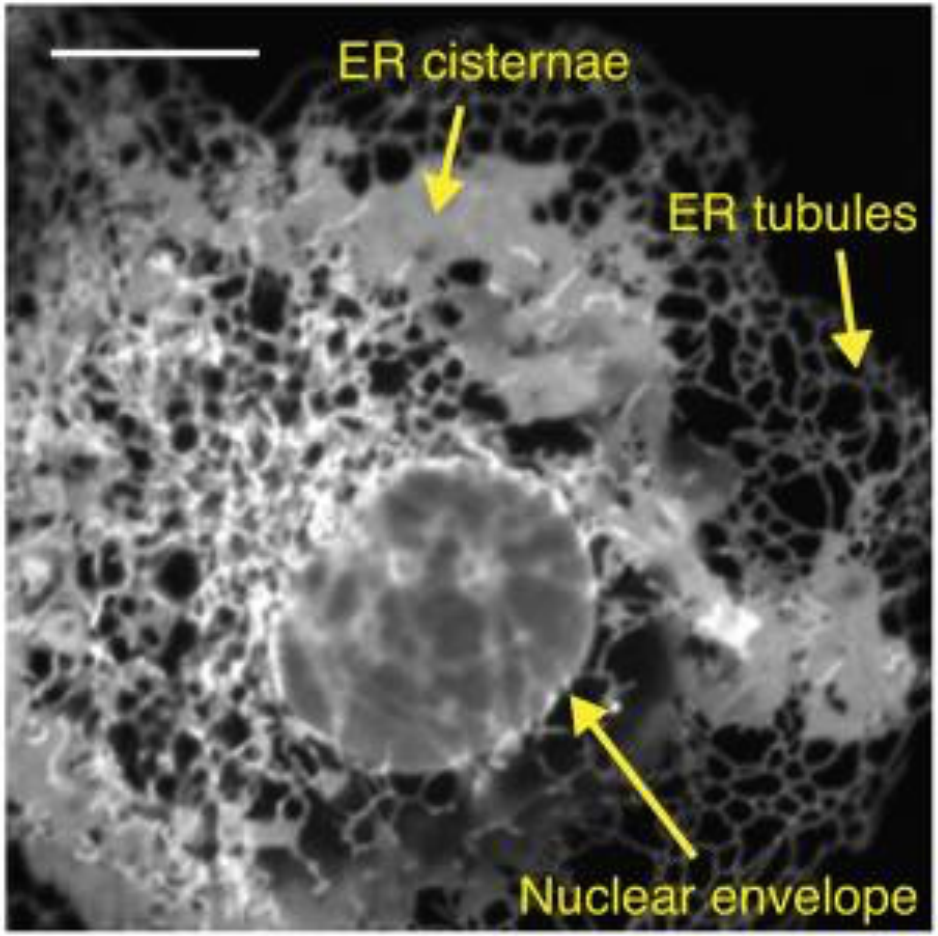

The continuous ER network morphology, co-existence of cisternal sheets and tubule forms. Changes in morphogenic protein density as well as strength and number of membrane-ER contact sites are known to induce interconversion.

Scale bar = 10μm.

Friedman & Voeltz, TICB-818 (2011)

Show animation

Endoplasmic Reticulum - Remodeling

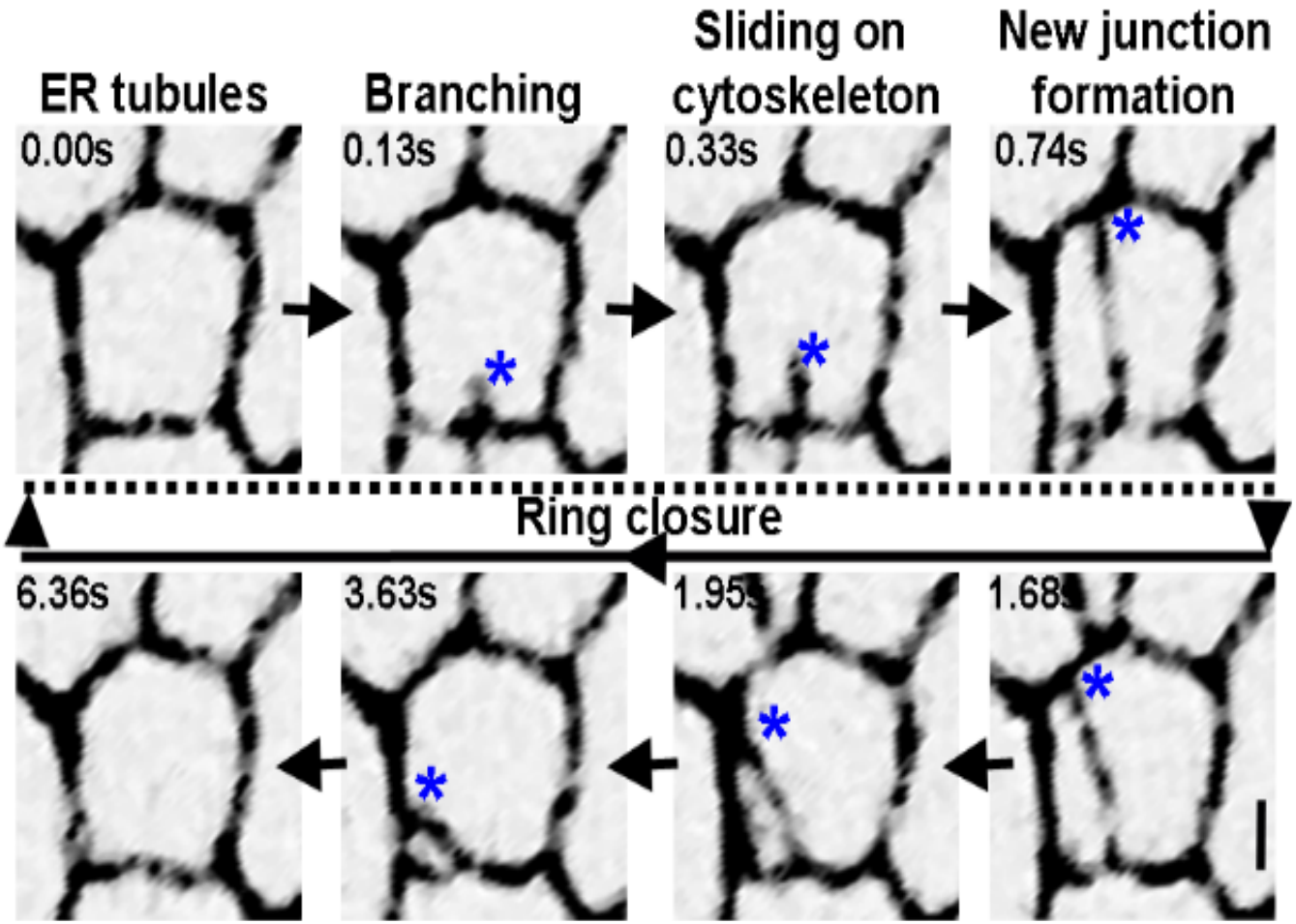

Budding and remodeling of the ER occurs on time scales of seconds, it involves purely co-dimension one interfaces (hollow tubules), and they almost never pearl. Griffing L. R. (2010)

ER - Loss of SHE1

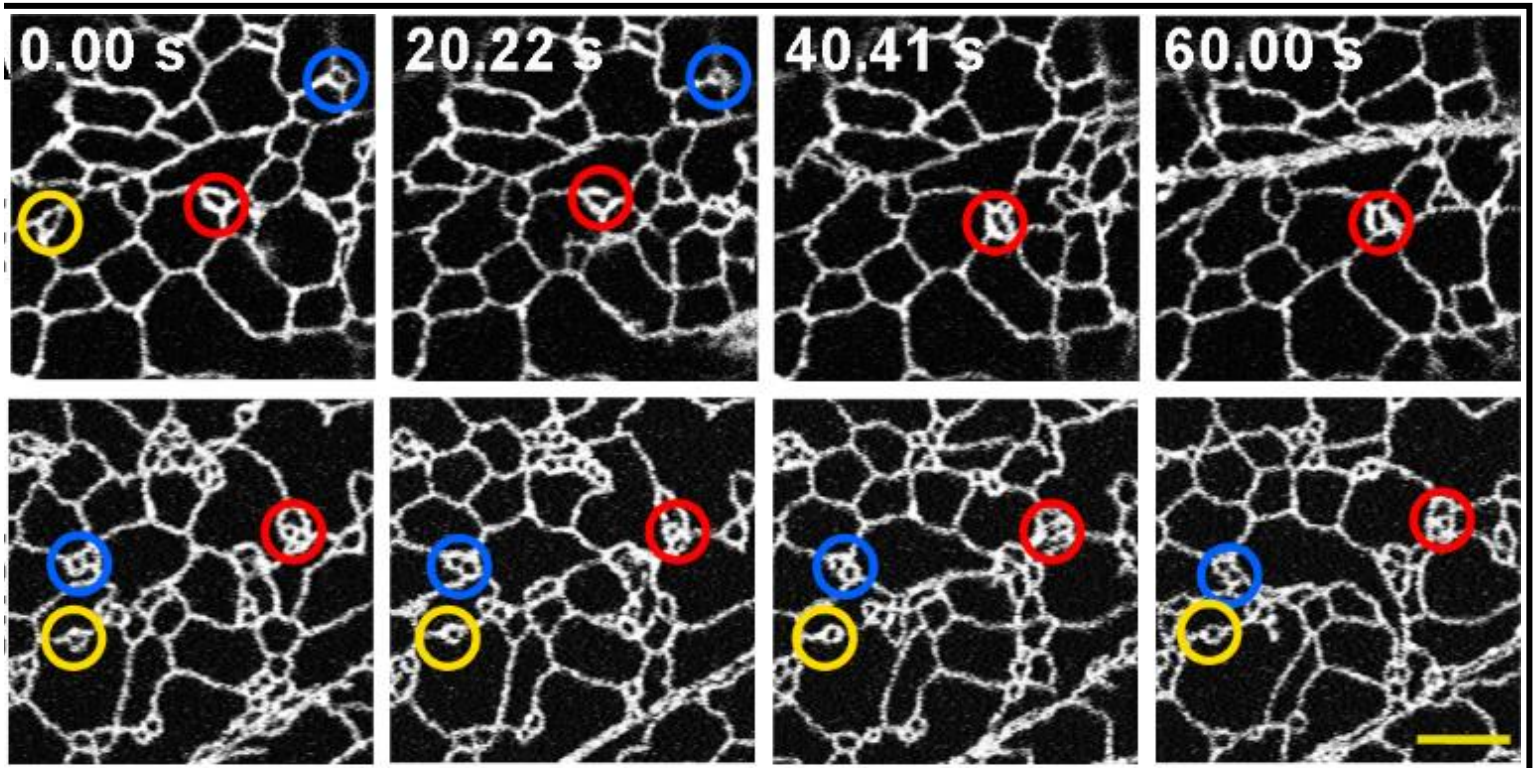

SHE1 is a microbial binding protein. Loss of SHE1 through genetic defect inhibits ER remodeling.

(top) Normal plant cell ER shows remodeling over 60 second.

(bottom) Cell with knocked-out gene does not remodel over same time period. Brandizzi F. (2014).

Bifurcation Diagram – Jain and Bates

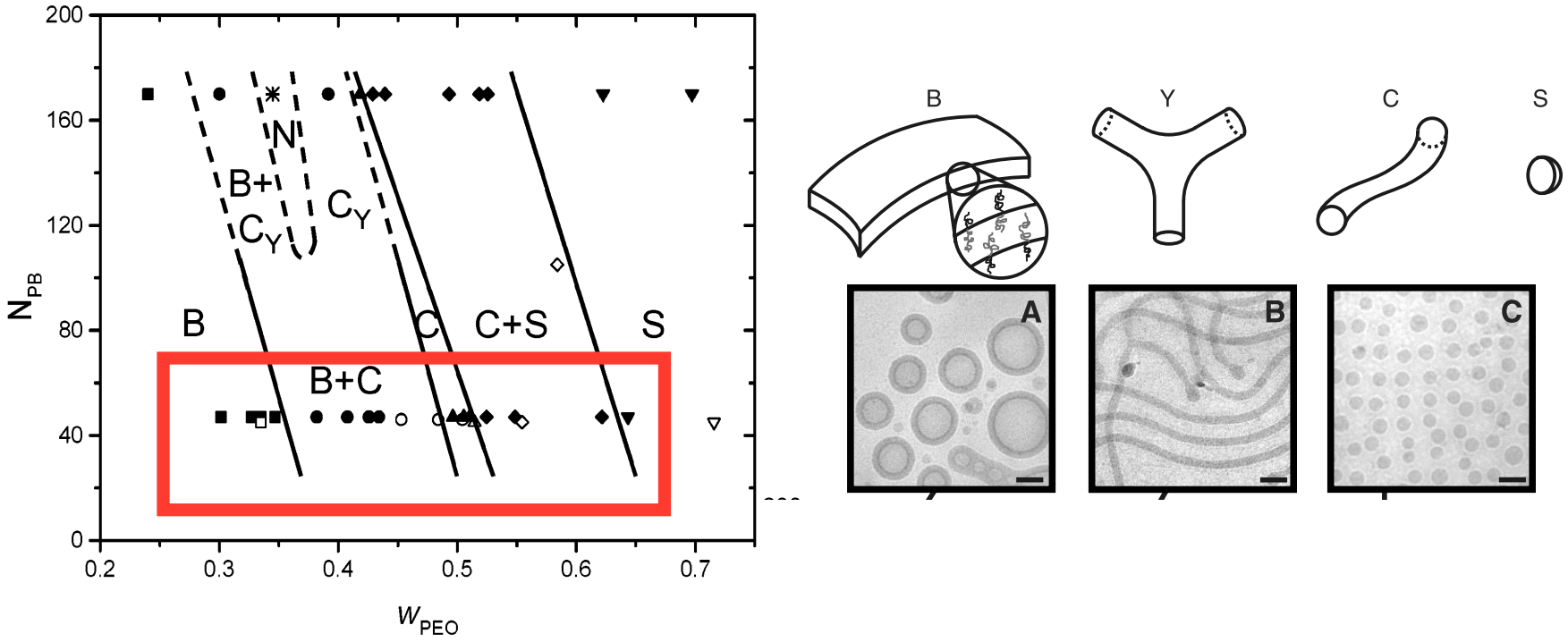

(Left) Bifurcation diagram for Polyethylene oxide (PEO) - Polybutadiene (PB) amphiphilic morphology as function of PEO weight fraction (horizontal axis) for fixed molecular weights of PB fixed at $N_{\mathrm{PB}} = 45$ and $\mathbf{170}$ (vertical axis). (Right) The shorter diblock shows the same codimensional bifurcation structure as Dicher and Eisenberg's change-of-solvent study. [Jain and Bates 2003].

Jain and Bates: Morphological Complexity

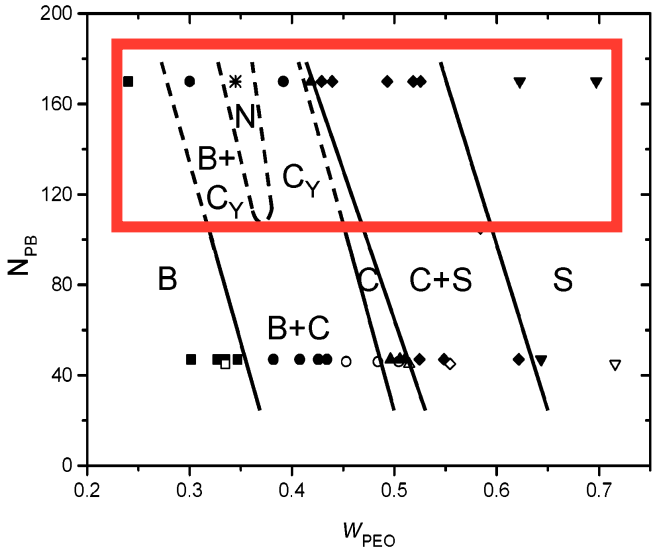

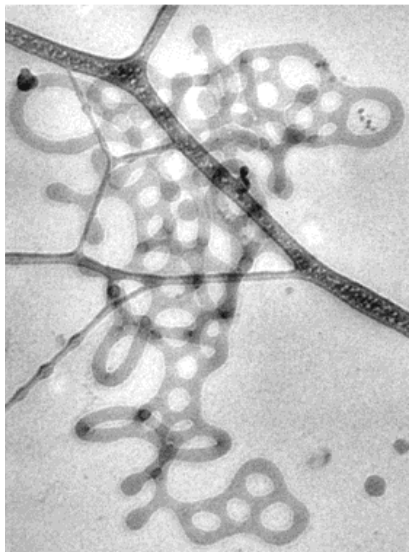

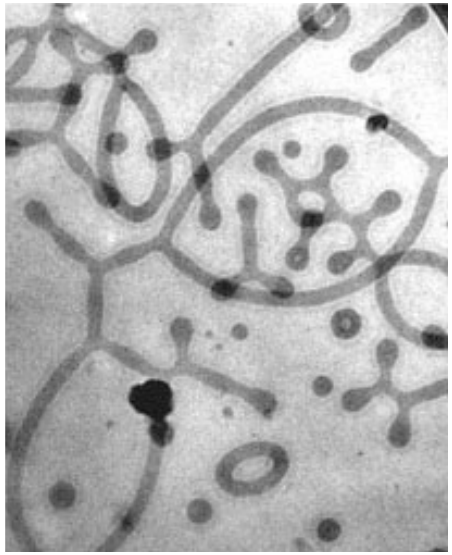

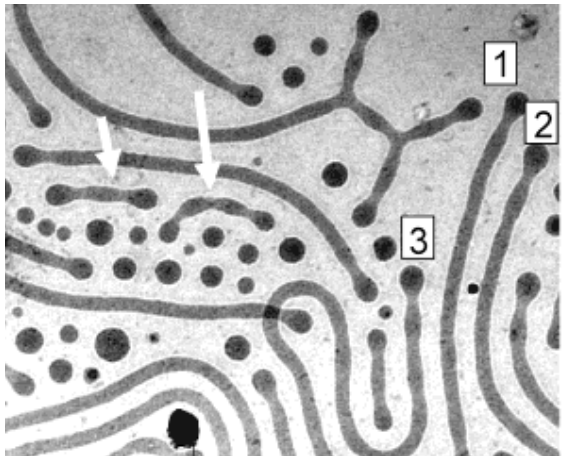

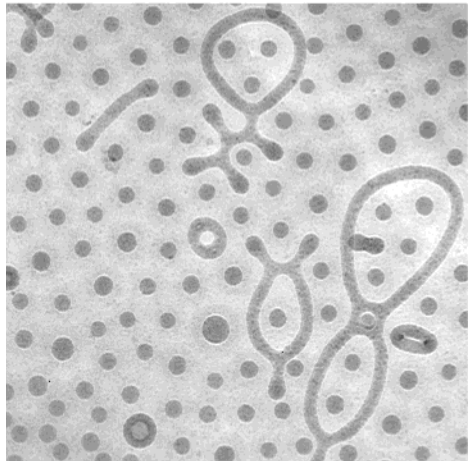

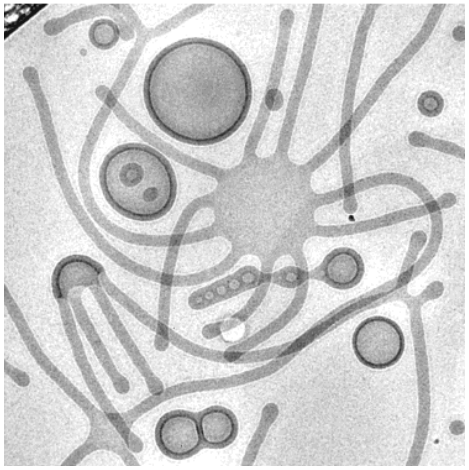

Longer PEO-PB diblock displays morphological complexity: pearled cylinders, networks, Y-junctions. Jain and Bates *Macromolecules* (2004).

Single Liquid: Amphiphilic Free energies

u volume fraction of amphiphile (lipid).

For amphiphilic mixtures: Tuebner & Strey (1987) Gompper & Schick (1990)

$$\mathcal{F}(u) := \int_\Omega \frac{\epsilon^4}{2}|\Delta u|^2 - \epsilon^2 G_1(u)\Delta u + G_2(u)\, dx,$$

any self-respecting Mathematician will complete the square

$$\mathcal{F}(u) := \int_\Omega \frac{1}{2}\Big(\epsilon^2\Delta u - \overbrace{G_1(u)}^{W'(u)}\Big)^2 - \overbrace{\boxed{\frac{1}{2}G_1^2 - G_2(u)}}^{P(u)}\, dx.$$

When $P \ll 1$, then the energy is very degenerate, very special.

$$\boxed{\mathcal{F}(u) = \epsilon^{-3}\int_\Omega \frac{1}{2}\left(\epsilon^2\Delta u - W'(u)\right)^2 - \delta\cdot P(u)\, dx.}$$

P tunes the tail packing-entropy and the solvent-head group electrostatics.

Functionalized Cahn-Hilliard Energy

$u - b_- > 0$ density of amphiphile. A distinguished limit $\delta = \epsilon^p$:

$$\mathcal{F}_{\mathrm{CH}}(u) = \epsilon^{-3} \int_\Omega \frac{1}{2}\left(\epsilon^2 \Delta u - W'(u)\right)^2 - \boxed{\epsilon^p \left(\frac{\epsilon^2 \eta_1}{2} |\nabla u|^2 + \eta_2 W(u) \right)} \, \mathrm{dx}.$$

$p = 1$ Strong Functionalization

$p = 2$ Weak Functionalization

Parameters: $\eta_1 > 0$ hydrophilic-solvent interaction, "solvent quality"

$\eta_2 \in \mathbb{R}$ aspect ratio and confinement of minority species

Well Parameters: tilt $W(b_-) - W(b_+)$, absorption rate $W''(b_-) > 0$, and lipid stiffness $W'(m_0)$.

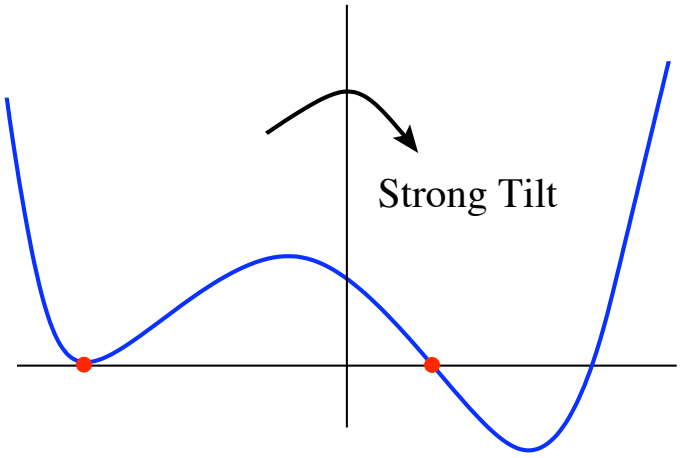

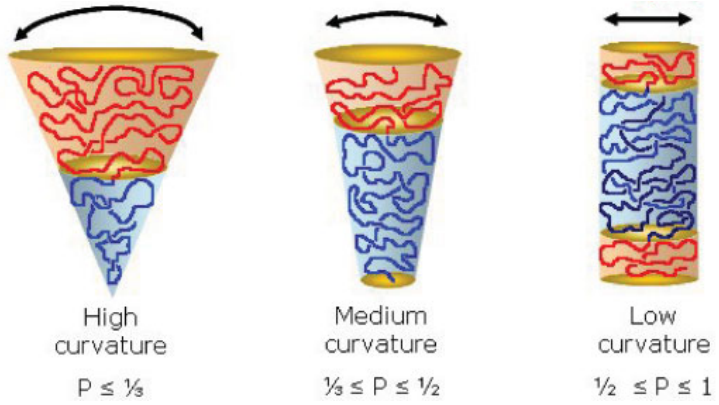

Bilayers: Co-Dimension One

Goal:

$$\text{Min} \int_\Omega (\epsilon^2 \Delta u - W'(u))^2 \, dx.$$

Near a codim one interface $\Gamma \subset \mathbb{R}^n$, the Laplacian becomes

$$\epsilon^2 \Delta = \partial_z^2 + \epsilon H \partial_z + \epsilon^2 \Delta_s$$

where H is the mean curvature of interface and Δ_s is Laplace Beltrami.

Look for $u = \phi(z)$:

$$\text{Min} \int_{\mathbb{R}} (\partial_z^2 \phi - W'(\phi) + \epsilon H \partial_z \phi)^2.$$

At leading order, the minimizer should solve the Lagrangian equation

$$\boxed{\left(\partial_z^2 - W''(\phi)\right)\left(\partial_z^2 \phi - W'(\phi)\right) = \Lambda} + O(\epsilon),$$

subject to $\phi \to b = b_- + \epsilon b_1$ as $z \to \pm\infty$.

Solve for Λ

$$\Lambda = \epsilon [W''(b_-)]^2 b_1,$$

Reformulate. H: Melnikov parameter; b_1: shape perturbation,

$$\partial_z^2 \phi - W'(\phi) = \epsilon \left(H \boxed{\partial_z \phi} + b_1 \boxed{[W''(b_-)]^2 (\partial_z^2 - W''(\phi))^{-1} 1} \right).$$

Spectrum of the Bilayer Dressing

For strong functionalization the bilayer dressing of hypersurface Γ:

$$u_b(x) := \phi_b(z) + \epsilon b_1(1 + \phi_{1,\mathrm{loc}}(z)) + O(\epsilon^2)$$

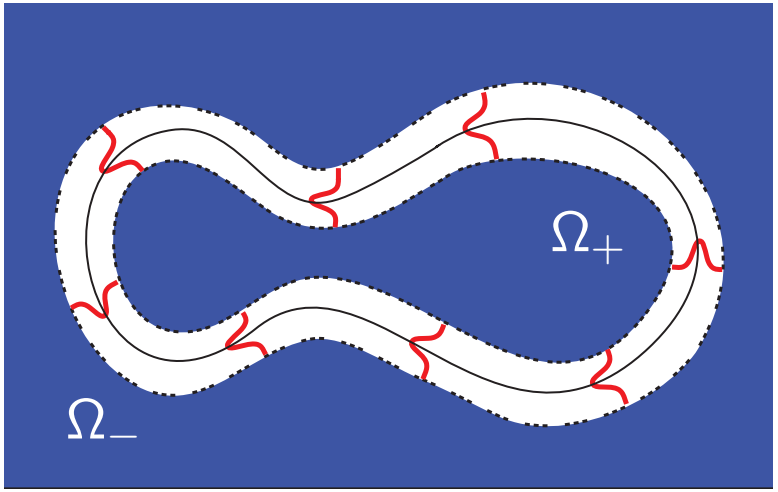

Stability of bilayers is determined by the eigenvalues of the second variation

$$\mathbb{L} := \frac{\delta^2 \mathcal{F}}{\delta u^2}(u_b) = \boxed{(\partial_z^2 - W''(\phi_b) + \epsilon^2 \Delta_s)^2} + O(\epsilon),$$

whose eigenfunctions separate to $O(\epsilon)$,

$$\Psi_{j,n} = \psi_j(z)\Theta_n(s) + O(\epsilon).$$

Functionalization = Multiple Quadratic curves of Eigenvalues

$$\mathbf{1D-inner} \qquad \mathbb{R}^n \qquad \mathbf{Functionalized}$$

$$L_0 = -\partial_z^2 + W''(\phi_b) \mapsto L = L_0 - \epsilon^2 \Delta_s \mapsto \mathbb{L} = L^2 + O(\epsilon)$$

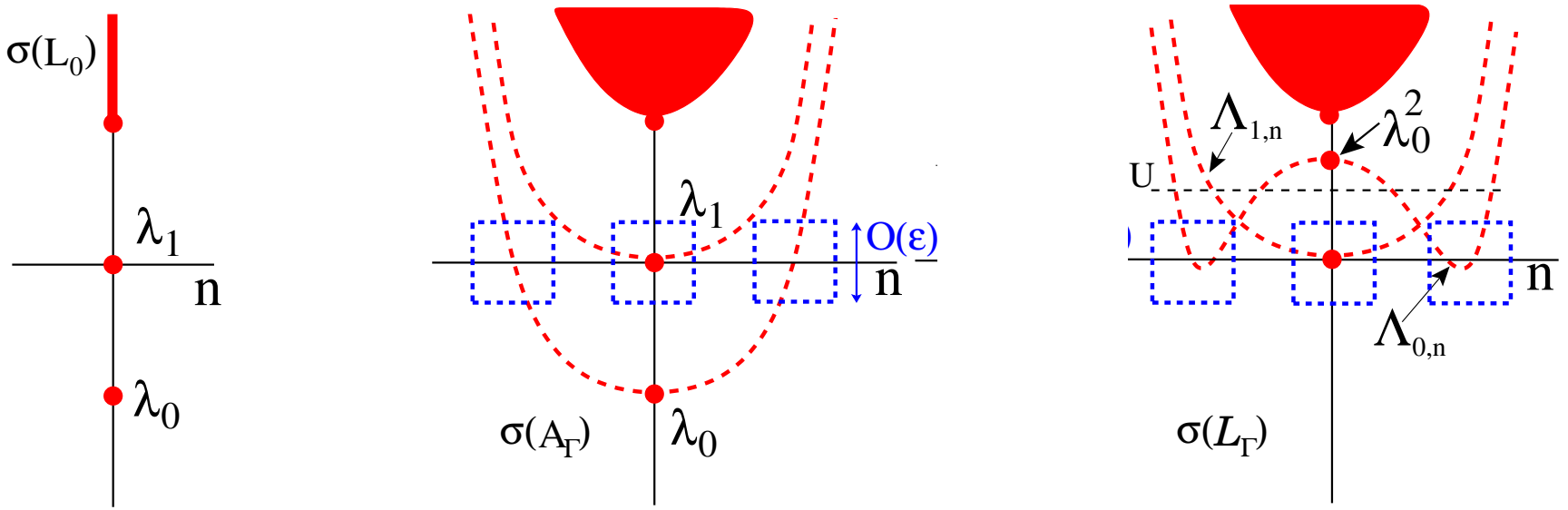

Characterize onset of Pearling:
P. and G. Hayrapetyan, *ZAMP* (2015)
Doelman, P., Wetton, Wu, *SIMA* (2015)
Kraitzman, P. *SIMA* (2018).

Existence of Pearled morphologies

P. and Q. Wu, *JDE* (2015)

Pearling Stability for Strong Functionalization

To talk to chemists, replace back-ground perturbation b_1 with perturbation of far-field chemical potential

$$\mu_1 := \frac{b_1}{W''(b_-)^2}.$$

Theorem: (Kraitzman, K.P.) [SIMA 2018] A dressing of an admissible bilayer is pearling stable iff

$$\mu_1 S_b + (\eta_1 - \eta_2)\lambda_{b,0} < 0,$$

and a dressing of an admissible filament is pearling stable iff

$$\mu_1 S_f + (\eta_1 - \eta_2)\left(\|\psi'_{f,0}\|^2 + \lambda_{f,0}\right) < 0.$$

Morphological Competition and Complexity

Consider the H^{-1} gradient flow of the free energy

$$u_t = \Delta \frac{\delta \mathcal{F}}{\delta u}(u) = \Delta \mu(u),$$

subject to periodic boundary conditions. On a $t = O(\epsilon^{-1})$ timescale, well separated bilayers and filaments in $\mathbb{R}^3$ evolve according to ϵ-scaled normal velocities

$$\boxed{\begin{aligned} V_{N,b} &= \nu_b(\mu_1 - \mu_b)H + \epsilon k_b \Delta_s H, \\ \vec{V}_{N,f} &= \nu_f(\mu_1 - \mu_f)\vec{\kappa} + \epsilon k_f \partial_s^2 \vec{\kappa}, \end{aligned}}$$

The sign of $\mu_1 - \mu_b$ determines if flow is **curve shortening** (negative) or **regularized curve lengthening** or "Meander" flow (positive).

In $\mathbb{R}^2$, bilayer normal velocity is equivalent to the flow of the 2nd fundamental form

$$H_t = -\left(\partial_s^2 + H^2\right)\left(\nu_b(\mu_1 - \mu_b)H + \epsilon k_b \partial_s^2 H\right).$$

The far-field chemical potential evolves to preserve total mass of amphiphile

$$\frac{d\mu_1}{dt} = -\frac{[W''(b_-)]^2}{|\Omega|}\left(\epsilon \int_{\Gamma_b} V_{N,b} H \, dS + \epsilon^2 2\pi \int_{\Gamma_f} \vec{V}_{n,f} \cdot \vec{\kappa} \, ds\right).$$

Show Movies

ER and Graphical Networks

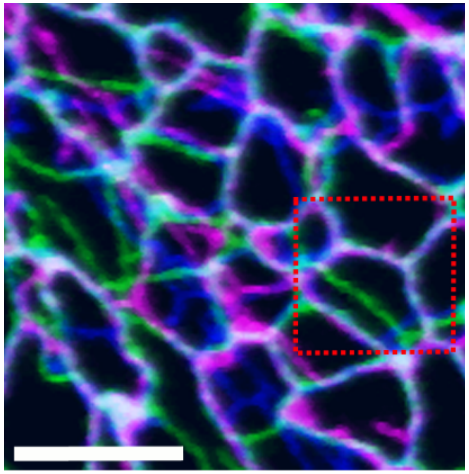

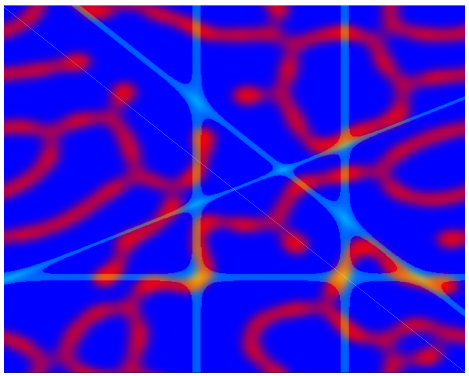

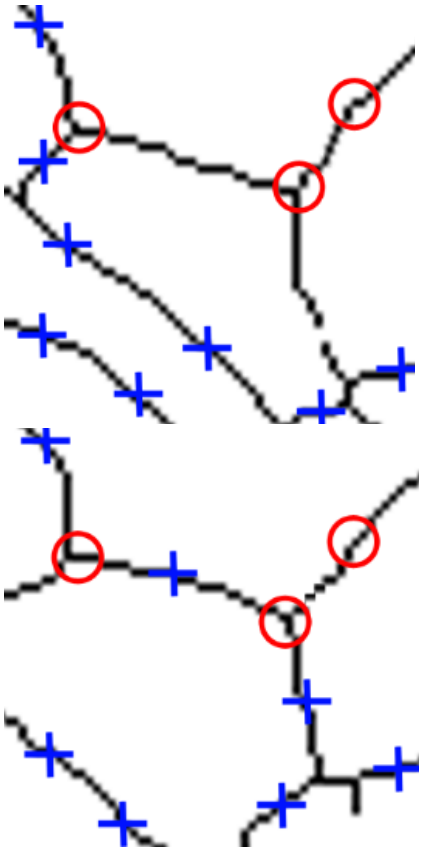

(Top left) Experimentally captured motion of reticulated tubular ER networks, three colors depict network at three distinct times, both fixed and mobile triple junctions are evident.
(bottom left) 2D simulation of gradient flow of FCH model with actin filaments (light lines).
(Right - top and bottom) Graphical network depiction of a subsection of the ER network showing fixed (circle) and mobile points (cross) at two different times.

Graphical network models miss mass transport limitations.

ER and Network Morphology

ER operates within the bilayer stability regime.

- Exchange of lipids with the bulk fluid is rare, $W''(b_-) \gg 1.$
- Lipids lipid mass/unit area of bilayers is fixed quantity $-W'(m_0) \gg 1.$
- Include location of "tethered" points pinning ER to plasma membrane $\eta_1 = \eta_1(x).$
- Lipids are produced/removed at various rates $G(u, \phi) \neq 0.$
- Protein density, $\phi = \phi(x, t)$, change packing preferences, intrinsic curvature, and connection properties. $\eta_2 = \eta_2(\phi), W = W(u; \phi)$

$$u_t = \Delta \frac{\delta \mathcal{F}}{\delta u}(u, \phi) + G(u, \phi),$$

$$\phi_t = \Delta \frac{\delta \mathcal{F}}{\delta p}(u, \phi).$$

Minimal ER model

What influence does slow growth/decay of lipid mass have on dynamics of ER network with fixed membrane contact points?

(No proteins yet)

ER - Loss of SHE1

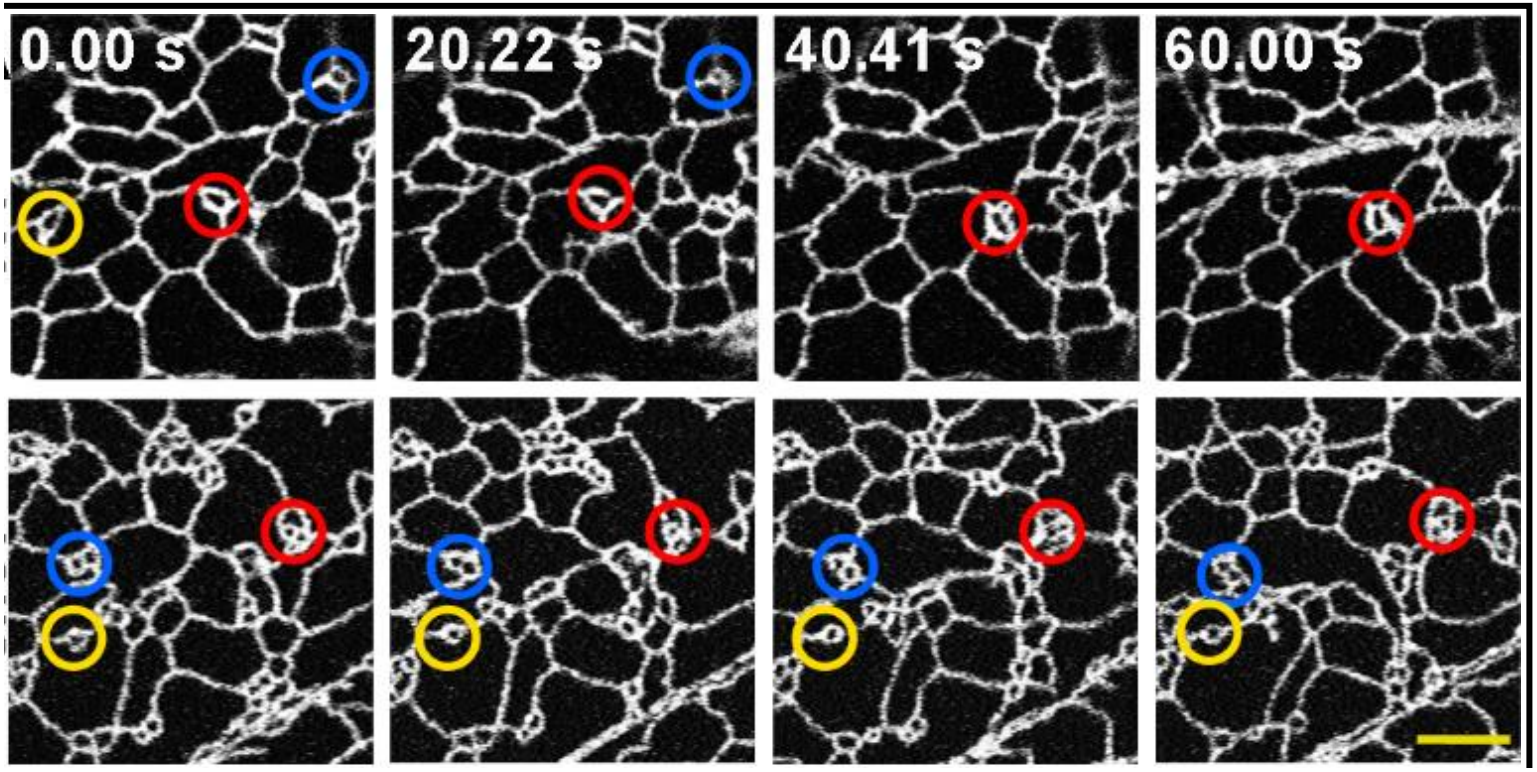

SHE1 is a microbial binding protein. Loss of SHE1 through genetic defect inhibits ER remodeling.

(top) Normal plant cell ER shows remodeling over 60 second.

(bottom) Cell with knocked-out gene does not remodel over same time period. Brandizzi F. (2014).

The ER: Morphogenic and Fusogenic surface proteins

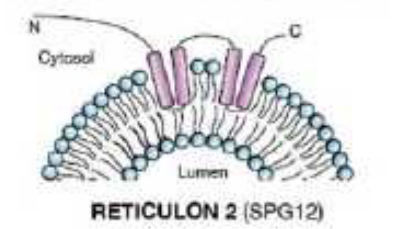

RETICULON 2 (SPG12)

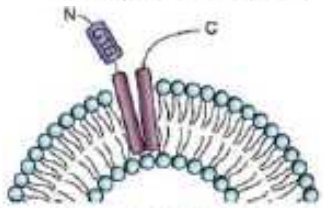

ATL1 (SPG3A, HSAN1), ATL3 (HSAN1)

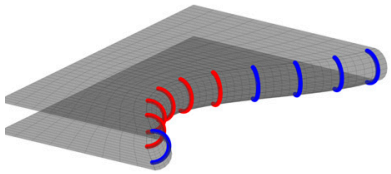

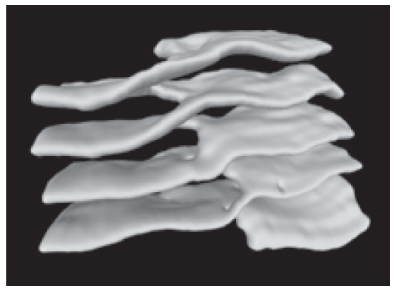

helical parking ramp

Surface proteins generically reside on the cytosolic side of the ER, not on the luminal side.

Reticulons: morphogenic, induce curvature **vectors**, typically one large and positive, one small and perhaps slightly negative. Have large role in fenestration.

Atlastin/RHD3: fusogenic proteins, play a key role in homotypic membrane fusion.

Spontaneous symmetry breaking:

spatial homogeneity through positive feed-back with large-curvature areas

in-plane symmetry through self-alignment of curvature vectors

through-plane symmetry distinguishes merging (luminal-luminal contact) from pinch-off (cytosolic-cytosolic contact) .

ER: Fenestration

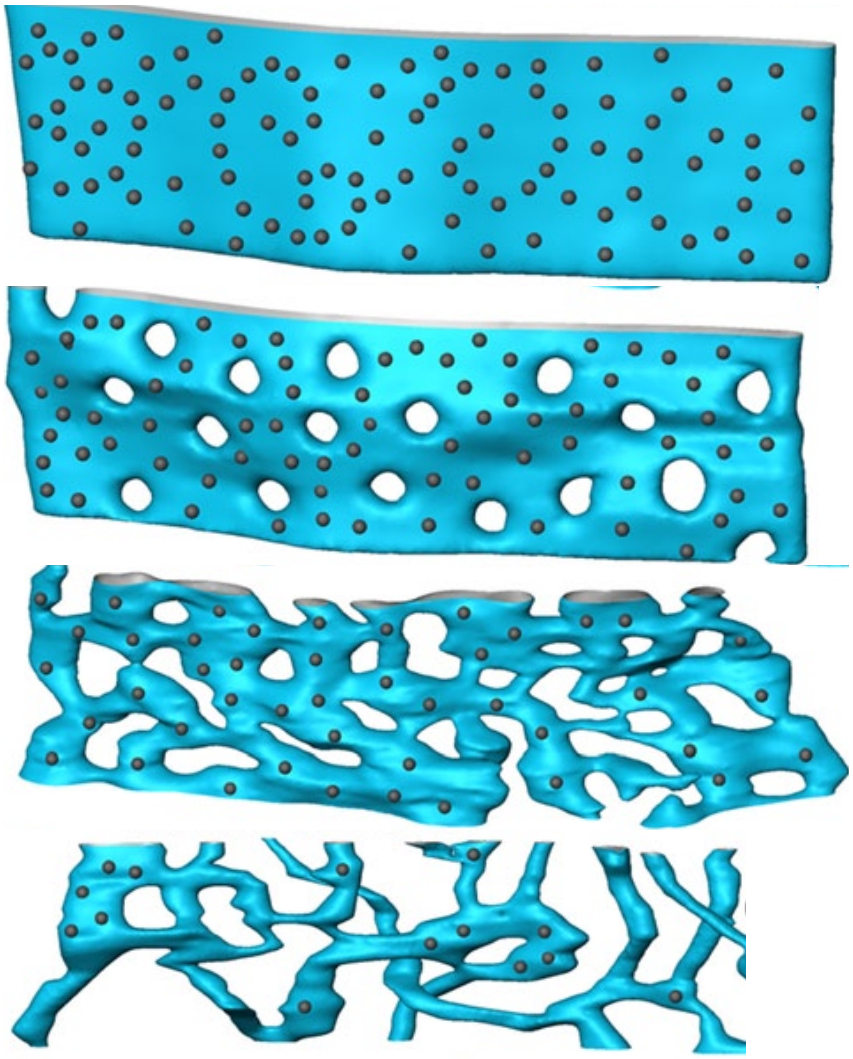

Fenestration (Latin: to create a window) A bifurcation mechanism for interconversion between cisternea and sheets. Induced by increasing density of reticulons. Simple models comparing energy of cisternae and tubule for blends of two types of reticulons – one with a small negative curvature – yield a plausible bifurcation diagram [Shemesh (2014)]

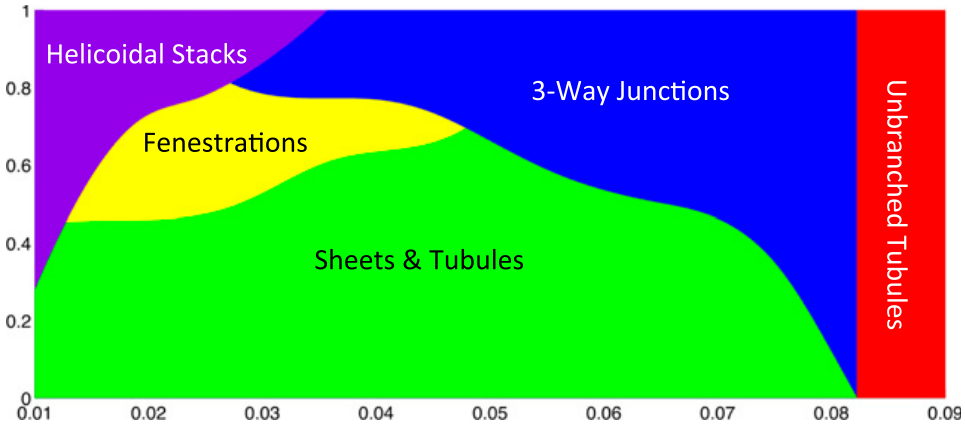

The FCH-Recticulon free energy

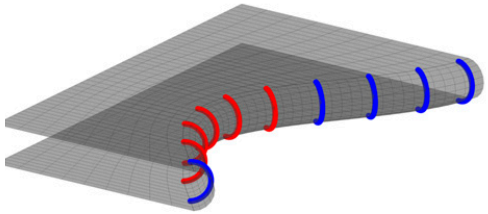

Morphogenic proteins induce targeted curvature vectors and interact dynamically with ER geometry. Consider two species of morphogenic proteins, with distinct densities $\phi = (\phi_1, \phi_2)$, but a common unit director vector, $\vec{n}_1$, that indicates the orientation of the proteins, and serves to break in-plane symmetry of the bilayer.

The second tangent-plane vector $\vec{n}_2 := \frac{\nabla u}{|\nabla u|} \times \vec{n}_1$, the coupling between the intrinsic curvature and the self-alignment, self-localization has the natural expression

$$\mathcal{R}(u, \phi, \vec{n}_1) := \frac{1}{\epsilon^3} \int_\Omega \Big(K_0 |\nabla u \cdot \vec{n}_1|^2 + D|\nabla \vec{n}_1|^2 + \epsilon D_0 e^{-\frac{u}{u_b}} |\phi|^2 + \boxed{\epsilon K_1 \sum_{k=1}^{2} \left| \vec{n}_k^t [\nabla^2 u] \vec{n}_k - \kappa_k(\phi) \right|^2} \Big) \, dx.$$

director: lies in tangent plane and self-align (spontaneously break symmetry)
proteins: absorb onto surface and couple to curvature

Morphogenic Proteins: surface sculpting

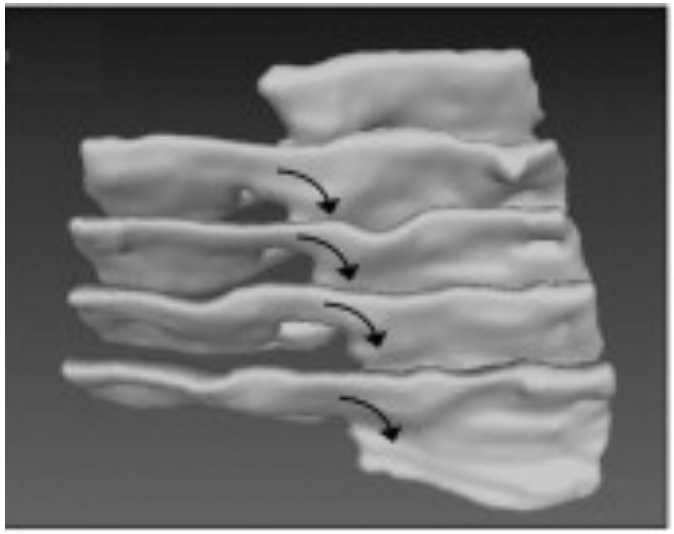

Terasaki et al **Cell** (2013)

$$u_t = \Delta\left(\frac{\delta \mathcal{F}}{\delta u}(u,\phi) + \frac{\delta \mathcal{R}}{\delta u}(u,\phi,\vec{n}_1)\right) + G(u,\phi),$$

$$\phi_t = \Delta \frac{\delta \mathcal{R}}{\delta p}(u,\phi,\vec{n}_1),$$

$$\partial_t \vec{n}_1 = \Pi^{\perp}_{\vec{n}_1} \Delta \frac{\delta \mathcal{R}}{\delta \vec{n}_1}.$$

Fusion-Fission Asymmetry

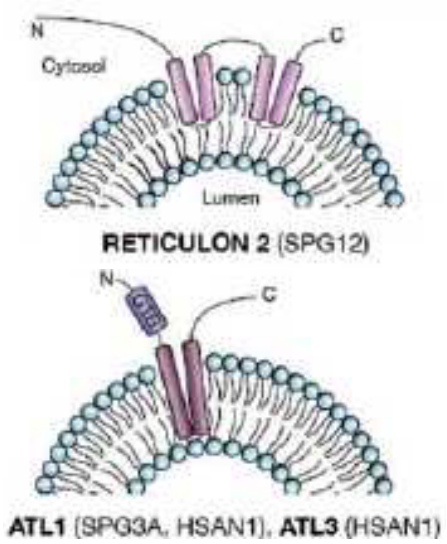

Key issue: Fusogenic proteins lie on the cytosolic leaf of the bilayer – there is a through-plane asymmetry (open-loop bilayer).

Key idea: It is much more stable, more efficient, to model a simpler bilayer composition and **two distinct fluids**. This is accurate as the cytosolic and luminal fluids have distinctly different compositions (luminal is Ca^{+2} rich). Three phases: a single lipid, and two fluids.

$$\left(D\partial_z^2 - \nabla_U G_1(U)\right)^t \left(D\partial_z^2 U - G_1(U)\right) = O(\epsilon).$$

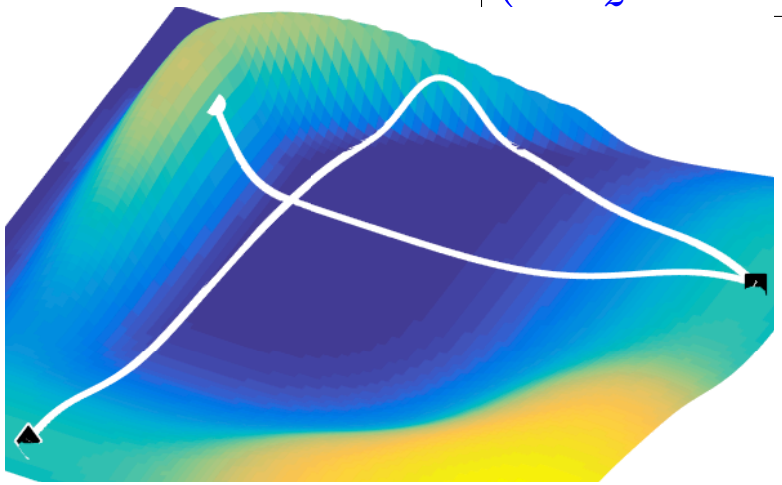

Billiard dynamics: Existence of multiple connections between cytosolic and luminal fluids as well as luminal-luminal homoclinics, but **not** cytosolic-cytosolic homoclinics. **Asymmetry embedded in "scattering potential"**.

Hemifusion

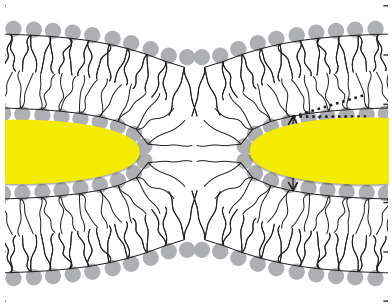

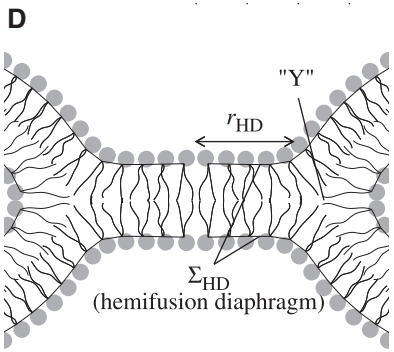

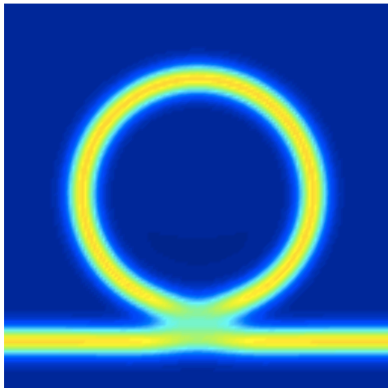

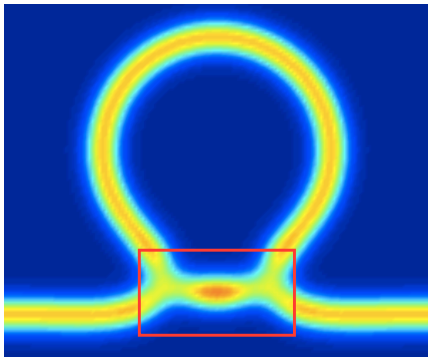

Ryham & Cohen (2016) used a liquid-crystal model for lipid bilayers to find minimal transition energies for stalk formation within the process of hemifusion.

The presence of fusogenic proteins (RHD3 in plants) greatly lowers the energy barrier for fusion of ER membranes, while not lowering the fission barrier.

Proteins control the existence of connecting orbits, and tune the values of energy barriers for “high energy” connections.

Existence of Connections and Barriers

The $4N$ dimensional dynamical system

$$\left(D\partial_z^2 - \nabla_U G_1(U)^\dagger\right)\left(D\partial_z^2 U - G_1(U)\right) = 0,$$

has a conserved quantity. All critical points of G_1, solutions to $G_1(p) = 0$ lie on the same $4N-1$ dimensional level set of the conserved quantity.

If $G_1(p) = 0$ and $\nabla_U G_1(p)$ has no strictly negative eigenvalues, then $p \in \mathbb{R}^N$ generates a normally hyperbolic fixed point of the $4N$ dimensional system, with $2N$ dimensional stable and unstable manifolds that lie on the $4N-1$ level set.

Conjecture: Any two normally hyperbolic critical points of G_1 have a connection within the $4N$ dimensional system. Any normally hyperbolic critical point has a non-trivial homoclinic connection.

- Under what conditions do these connections reside within the $2N$ dimensional zero-energy system?
- How do we tune their distance to the $2N$ dimensional system?

MultiComponent Models with Energy Barriers

Zero-energy connections are k-dimensional manifolds within the sub-system

$$D\partial_z^2 U - G_1(U) = 0,$$

subject to $U(z) \to p_\pm$ as $z \to \pm\infty$.

A Homoclinic Barrier to $p \in \mathbb{R}^N$ is a $k \leq N$-dimensional manifold $\mathcal{M}$ within the full system

$$\left(D\partial_z^2 - \nabla_U G_1(U)^\dagger\right)\left(D\partial_z^2 U - G_1(U)\right) = 0,$$

subject to $U(z) \to p$ as $z \to \pm\infty$, with the constraint that each solution U on the barrier solves

$$D\partial_z^2 U - G_1(U) = \alpha\Psi, \tag{1}$$

where $\Psi \in \mathrm{Ker}(D\partial_z^2 - \nabla_U G_1(U)^\dagger)$ has norm 1 and $|\alpha| > 0$ is constant on connected components of $\mathcal{M}$.

The Melnikov parameter α measures the 'energy' required to bend the stable and unstable manifolds of p within $2N$ dim system to intersect along U. (1) implies

$$\int_{\mathbb{R}} |D\partial_z^2 U - G_1(U)|^2 \, dz = \alpha^2.$$

MultiComponent Models with Energy Barriers

Characterize potentials $G_1 : \mathbb{R}^2 \mapsto \mathbb{R}^2$ with

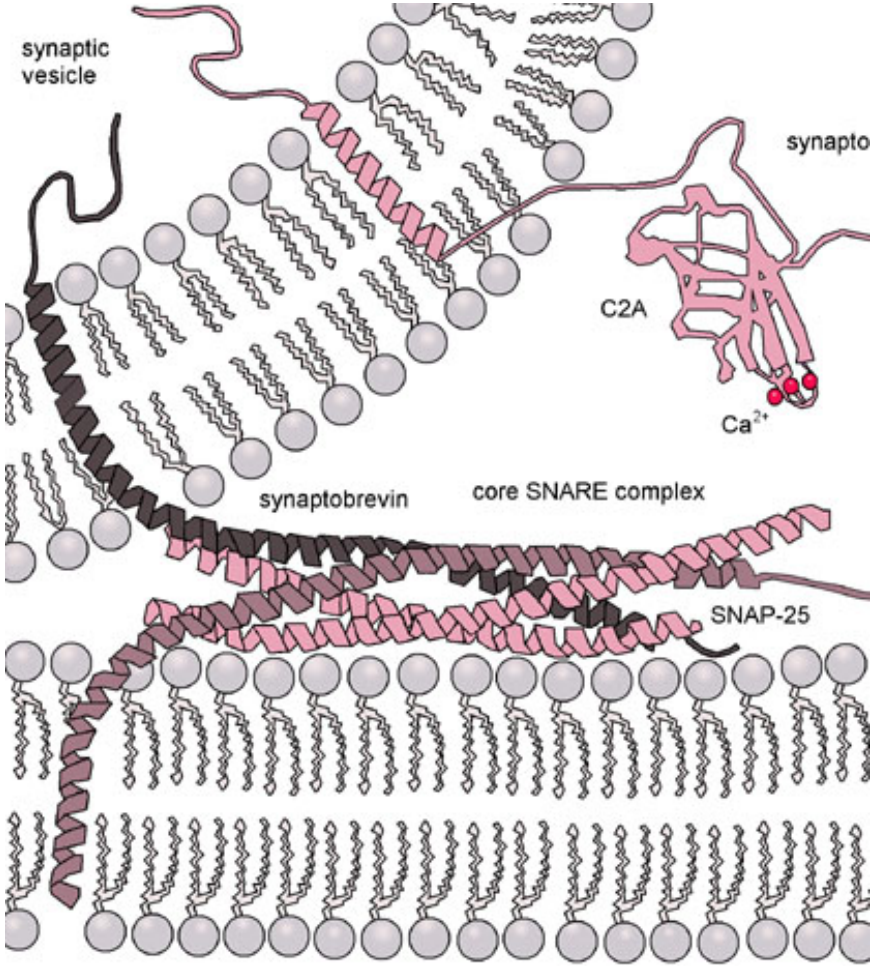

- Hyperbolic fixed points p_1 and p_2 with zero-energy connection between (p_1, p_2).
- The linearized operators associated to this connection contains no strictly positive eigenvalues.
- The homoclinic barriers to p_1 and p_2 have energies α_1 and α_2 that are independently tunable, down to zero. Proteins tune the value of this energy barrier.

Snare proteins facilitate membrane fusion.

Acknowledgments

NSF-DMS 1409940
NSF-MCB 1714561
(PI-Brandizzi)
NSF-DMS 1813203